JOURNAL OF MATERIALS SCIENCE 7 (1972) 84–92

The Tensile Properties of a Superplastic Aluminium Bronze

G. L. DUNLOP
Department of Metallurgy, University of Cambridge, UK

D. M. R. TAPLIN
Department of Mechanical Engineering, University of Waterloo, Waterloo, Ontario, Canada

The high temperature tensile properties of a micrograin Cu-9.5% Al-4% Fe alloy, which is superplastic at 800°C, have been determined. Elongations at fracture of greater than 700% are achieved when the nominal strain-rate is in the range 3.9×10^{-2} min^{-1} to 7.9×10^{-2} min^{-1}. The nature of plastic instability in superplastic materials is considered and it is shown that the amount of strain at the onset of plastic instability is inversely related to the applied strain-rate and is relatively independent of the strain-rate sensitivity exponent, *m*. The onset of plastic instability during a tensile test results in an increase of local strain-rate at the point of minimum cross-section and this, together with the existence of a triaxial stress state in the necked region, may produce errors in the *m* versus strain-rate plot if *m* is determined by the change-rate method. The initial strain-rate for maximum elongation is lower than the strain-rate for maximum *m*. This may be ascribed either to the influence of plastic instability or the formation of cavities at the higher strain-rates.

1. Introduction

The purpose of this paper is to present and discuss the tensile properties of a micrograin aluminium bronze which is superplastic [1, 2] at 800°C and also to present new information regarding the necking behaviour of strain-rate sensitive materials. The aluminium bronze (CDA Alloy 619) which has a nominal composition of Cu-9.5% Al-4% Fe was developed by Olin Corporation as a high strength, oxidation resistant material [3]. The microstructure and microstructural changes which occur during superplastic deformation of this alloy, the influence of alloying content and temperature on the superplastic properties, and the anisotropic ductility are to be described elsewhere [4, 5]. Only a small amount of work on micrograin superplastic copper alloys has previously been published [6, 7] although phase transformation superplasticity in α/β and β/β' brasses has received considerable attention [1]. Of interest in the present study is that micrograin superplasticity is observed in an alloy which is close to a eutectoid composition although the temperature of the study is considerably higher than the eutectoid temperature so that the alloy is in the two phase ($\alpha + \beta$) field with a fine duplex microstructure stabilised by iron-rich particles [5]. This is in contrast to most other superplastic eutectoid alloys where advantage is made of the eutectoid transformation to provide a fine stable microstructure which is superplastic at temperatures just below the eutectoid temperature [1, 2].

Superplastic materials usually separate in tension by the simple growth of a neck until approximately 100% reduction in area is reached (intrinsic plastic failure) [8]. The total plastic strain at fracture is the sum of the uniform strain at the commencement of plastic instability e_u, and the strain subsequent to the onset of instability, e_{neck}. The magnitude of each of these strains, and so the total fracture strain is dependent on the resistance of the material to plastic flow. In general, for metals this resistance may be expressed in the constitutive equation:

$$\sigma = \sigma_y + k \epsilon^n \dot{\epsilon}^m \qquad (1)$$

where σ is the flow stress, σ_y is a yield stress, k is a constant, ϵ is strain, $\dot{\epsilon}$ is strain-rate, n is the strain-hardening exponent and m is the strain-

rate sensitivity exponent. Under high temperature conditions where diffusion is rapid, σ_y is close to zero, since at an infinitesimal "zero" strain-rate the initial flow stress approaches zero because only a very small finite stress is necessary to cause a metal to flow by atomic diffusion [9]. Equation 1 then reduces to:

$$\sigma = k \epsilon^n \dot{\epsilon}^m \quad (2)$$

In a tensile test, plastic instability occurs at the stage when maximum load is reached at which strain hardening effects, due to the effect of the test on material properties, are offset by geometrical softening due to the reduction of cross-sectional area. For a non-viscous material, where $m = 0$, e_u is shown by Considère's construction [10] to be equal to n. For a linear viscous material exhibiting no work hardening ($n = 0$ and $m = 1$) plastic instability does not occur [11, 12]. Campbell [13] has predicted that for a non-linear viscous material ($n = 0$, $0 < m < 1$) that e_u should increase with decreasing strain-rate and with increasing m. In partial corroboration of this, Wray [14] has found experimentally that for strain-rate sensitive materials the strain at which plastic instability commences can be postponed by decreasing the strain-rate.

Superplastic materials are characterised by very low values of n [15, 16] and values of m in the range 0.4 to 0.8 at strain-rates under conditions where ductility is a maximum [1, 2, 8] so that for these materials equation 2 can be reduced to:

$$\sigma = k \dot{\epsilon}^m \quad (3)$$

Successive workers have demonstrated that the extreme ductility achieved during superplastic flow is a result of the retarding influence of relatively high values of m on the growth of necks, [8, 17-20]. However, Wray [14] has shown experimentally that in such semi-viscous materials the magnitude of e_{neck} may not necessarily be controlled by the steady growth of one neck until point separation but rather may be governed by a second stage of instability whereby one neck, amongst a series of necks developing simultaneously, becomes increasingly active at the expense of the activity of the other necks. This increased activity of one neck then leads to intrinsic plastic failure. Morrison [20] has shown that the tendency for several necks to develop along the gauge length of strain-rate sensitivity materials is a function of specimen geometry. Multiple necking was found to occur in specimens of round cross-section when the diameter to gauge length ratio was less than 0.1. It has not been shown whether the second stage of plastic instability leading to intrinsic plastic failure occurs under circumstances where only one neck forms in the gauge length. However, since it is difficult to envisage how the presence of adjacent necks can affect the growth of a neck which is responsible for failure, it seems likely that the two stage instability behaviour may occur independently of the total number of necks present.

The importance of these features of unstable flow in strain-rate sensitive materials is emphasised in the present study.

2. Experimental

Alloy 619, of the composition shown in table I was supplied as 1 mm thick cold rolled sheet and 8 mm thick hot rolled plate. Flat specimens of 12.7 mm gauge length, 9.5 mm gauge width and 1 mm thickness and round cross-section specimens of 16.1 mm gauge length and 4.5 mm diameter were machined from sheet and plate materials respectively with the tensile axes parallel to the rolling direction.

TABLE I Chemical composition of Alloy 619

Aluminium	9.5%
Iron	4.0%
Zinc	0.8% max.
Lead	0.01% max.
Total other impurities	0.01% max.
Copper	Balance

Tensile testing was carried out in air at elevated temperatures at nominal strain-rates in the range 4×10^{-3} min^{-1}, to 4 min^{-1}, on Instron testing machines fitted with vertical split tube furnaces. Temperatures along the gauge length of flat specimens were maintained within $\pm$ 2°C of the test temperature during each test. For round cross-section specimens a temperature differential of up to 10°C could arise along the gauge length during each test. After inserting the specimen the furnace was brought up to the testing temperature in about 20 min. and held at that temperature for 30 min before setting the cross-head in motion. The strain-rate sensitivity (m) was determined by a change-rate procedure due to Backofen [8] and also by determining the tangential slope of log stress versus log strain-rate

curves. At the completion of tensile tests elongation measurements were made on the total specimen length since the demarcation between shoulder regions and gauge length became indistinct after straining. Considerable strain occurred outside the gauge length and so strain values are over-estimated. Internal stresses developed during tensile deformation at 800° C were determined by a modified relaxation technique suggested by Lloyd and Embury [21]. Each internal stress determination was accomplished within approximately 30 sec of stopping the cross-head motion of the Instron testing machine and was calculated on the basis of the final cross-section area.

3. Results and Discussion

3.1 Sheet Material

The effect of temperature on peak values of m as determined by the change rate method is recorded in table II from which it is clear that 800° C is the optimum temperature for superplasticity. At all temperatures, the strain-rate for peak m was approximately 3×10^{-2} min^{-1}. This contrasts with most other alloy systems in which superplasticity has been found since peak m usually occurs at increasing strain-rates as the temperature is increased [2]. In the present case it is of relevance that the distribution of phases within the microstructure varies with temperature – the proportion of α phase to β phase decreasing with increasing temperature [22]. At 800° C these phases are present in equal amounts. The strong dependence of fracture elongation on m, noted by other workers [1, 2] is confirmed in table II. Maximum elongation for a nominal strain-rate of 3.9×10^{-2} min.$^{-1}$ occurred at 800° C and was greater than 770% (the limit of cross-head travel). A similar effect of substantially increased ductility at a corresponding strain-rate at 800° C has been noted by Tyler and Goodwin [24] in alloys of similar composition but containing 5% Ni. However, the authors did not associate their observation with superplasticity.

TABLE II Effect of temperatures on peak values of m and elongation at fracture at a nominal strain-rate of 3.9×10^{-2} min^{-1}.

Temperature, °C	Peak m	Elongation, %
600	0.38	32
700	0.40	75
750	0.48	150
775	0.52	325
800	0.64	> 770
825	0.56	290
900	0.20	40

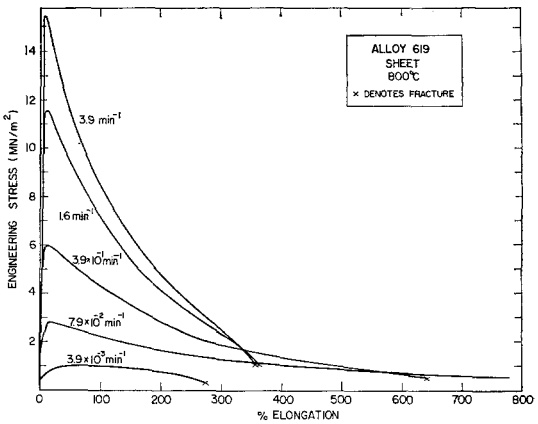

Figure 1 Typical engineering stress-strain curves for a range of strain-rates 800° C (sheet material).

Tensile tests of flat specimens at 800° C produced nominal stress-strain curves; some of which are recorded for a range of initial strain-rates in fig. 1. At initial strain-rates of 3.9×10^{-2} min^{-1} and 7.9×10^{-2} min^{-1} maximum elongations of 770% without fracture (the limit of cross-head travel) were obtained. A minimum elongation at fracture of 280% occurred when the lowest initial strain-rate of 3.9×10^{-3} min^{-1} was employed, while at the maximum initial strain-rate of 3.9 min^{-1} an elongation at fracture of 380% was recorded.

The elongation at the onset of plastic instability, as determined by the point of maximum load in the tensile test, was found to make a relatively small contribution to the total elongation at most strain-rates but was also found to increase with decreasing strain-rate (fig. 2) as predicted by Campbell [13] and Wray [14]. It should be noted that the strain at the onset of necking may not necessarily follow the same dependence on strain-rate as the point of maximum load which defines the onset of plastic instability. Wray [14] has shown that necks begin to grow from well before the strain when maximum load is reached in strain-rate sensitive In-Pb alloys while Keeler [23] only found obvious necking at strains approximately three times that for maximum load in cold rolled Zr tested at 200 to 300° C.

The magnitude of maximum engineering stress showed a marked variation with strain-rate over

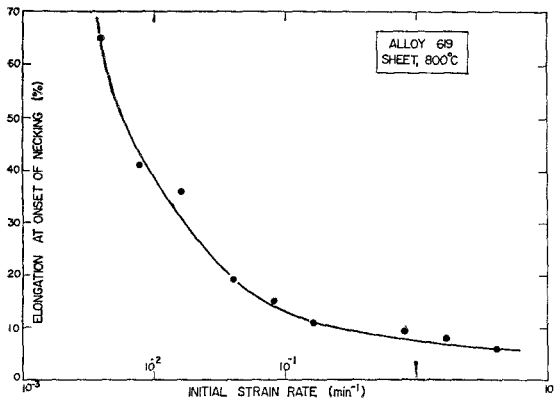

Figure 2 Elongation at the onset of plastic instability as a function of the initial strain-rate.

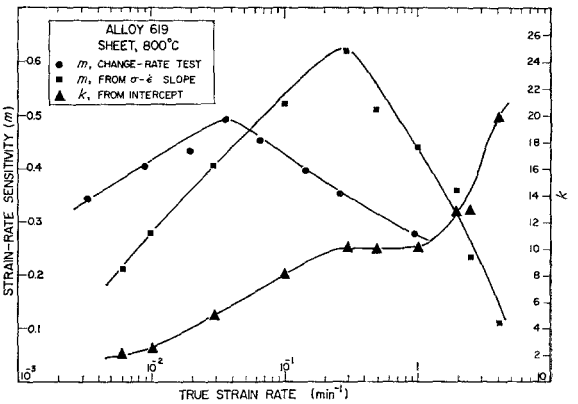

Figure 4 The effect of strain-rate on the strain-rate sensitivity exponent as determined by two different methods and the effect of strain rate on the coefficient K.

an intermediate range of strain-rate indicating a high strain-rate sensitivity of the flow stress in this region. This effect is recorded as a plot of log stress versus log strain-rate in fig. 3. An offset proof stress proved difficult to measure so maximum engineering stress was chosen for the flow stress parameter.

Values of m (defined by equation 3 as the slope of a $\log\sigma - \log\dot{\epsilon}$ plot) were determined from fig. 3 and are plotted in fig. 4 as a function of strain-rate. Values of k determined from intersections of lines drawn tangential to the curve in fig. 3 at the approximate strain-rate with the vertical $\log\dot{\epsilon} = 0$ line, are also plotted in fig. 4 together with values of m determined by the change rate method. There is a considerable difference between the values of m determined by the two methods and the strain-rates at which peak values of m occur. The peak value of m determined from the $\log\sigma - \log\dot{\epsilon}$ slope was 0.64 while the corresponding value for the change rate method was 0.5. Similarly peak values of m determined from the $\log\sigma - \log\dot{\epsilon}$ slope were recorded at a strain-rate which was an order of magnitude greater than for the corresponding peak determined by the change rate method. It has been suggested previously that erroneous values of m determined by change-rate tests may result from microstructural coarsening [23]. In the present case, little grain growth occurred during testing and it is most likely that the disparity between the $m - \dot{\epsilon}$ curves determined by the two methods arises because the results of change-rate tests are influenced by the necking behaviour of the tensile specimen. Values of m at each change of cross-head speed were associated with the average "true" strain-rate, between the two speeds, computed on the basis of uniform

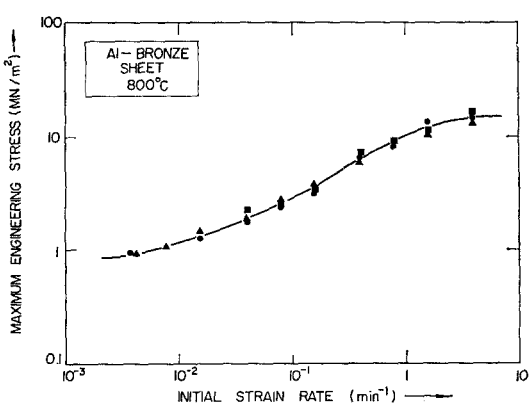

Figure 3 Maximum engineering stress as a function of the initial strain-rate.

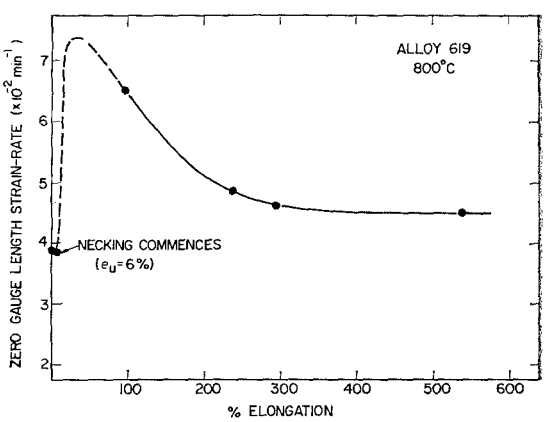

Figure 5 The variation of local strain-rate of the point of minimum cross-section with elongation (initial strain-rate 3.9×10^{-2} min^{-1}).

elongation. That is, it was assumed that the radius of curvature of the neck was so large that the influence of necking on local strain-rates could be considered negligible. This assumption is examined in fig. 5 in which local strain-rates at the point of minimum cross-section have been estimated for several strains at an initial strain-rate of $3.9 \times 10^{-2}\,\text{min}^{-1}$. The calculated points in fig. 5 result from minimum cross-sectional areas measured on several specimens from interrupted tensile tests. Since true strain is given by:

$$\epsilon = \ln (1 + e) \tag{4}$$

and since zero gauge length engineering strain is defined by:

$$e_z = \frac{L - L_0}{L_0} = \frac{A_0}{A} - 1 \tag{5}$$

where L_0, L, A_0 and A are the initial and final gauge length, and initial and final cross-sectional areas respectively; then the zero gauge length true strain-rate is

$$\dot{\epsilon}_z = \frac{\mathrm{d} \ln \frac{A_0}{A}}{\mathrm{d}t}$$

Zero gauge length strain-rates, $\dot{\epsilon}_z$, were calculated from the slope of a plot of ϵ_z versus time. The sharp increase in local strain-rate just after the onset of necking, suggested by fig. 5 implies that the local strain-rates developed in a change-rate test may be significantly greater than estimated by assuming uniform elongation. This may be particularly so when it is considered that all rate changes were made at less than 100% elongation. The lack of uniformity of flow along the gauge length of necking superplastic tensile specimens suggests, contrary to recent suggestions [25, 26], that there is little to gain from substituting "constant true strain-rate" (on the basis of uniform elongation) tensile tests for the more common constant cross-head speed tests in the testing of superplastic materials.

In fig. 6 true stress is plotted against zero gauge length true strain for the same set of interrupted tests used in fig. 5. The dashed line of fig. 6 is the computed stress which should arise in simple uniaxial tension assuming that equation 3 is a suitable constitutive equation and using $\dot{\epsilon}_z$ data from fig. 5, m data ($\log\sigma - \log\dot{\epsilon}$ slope) and k data from fig. 4. The increasing

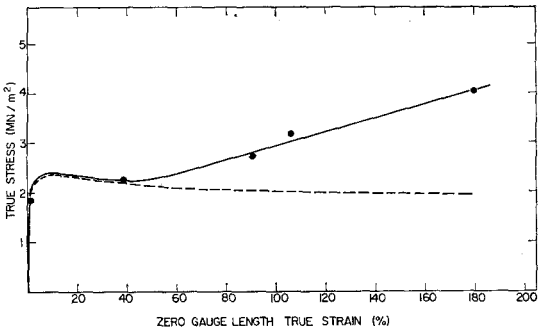

Figure 6 Apparent true stress—true strain curve using data from the same specimens as fig. 5. The dashed line indicates the stress which should arise assuming $\sigma = k\dot{\epsilon}^m$.

difference with increasing strain between the full and dashed curves of fig. 6 could arise from either strain hardening or the influence of a triaxial stress state. Previous workers [16, 27] found little or no strain-hardening to occur during superplastic deformation of the alloys although Watts and Stowell [25] found flow stress to increase with strain in the Al-Cu eutectic and ascribed this to strain enhanced grain growth. In the present case transmission electron microscopy has indicated that a stable dislocation sub-structure which could cause some strain-hardening is produced at this strain-rate and only a small amount of grain growth occurs [5]. It is likely that the apparent rise in flow stress is partially due to strain-induced hardening and also partially due to the development of a triaxial stress state in the specimens following necking.

The Bridgeman correction [28] for obtaining a uniaxial stress equivalent to the triaxial stress state in necked cylinders has been found to be inadequate under high temperature conditions where the flow stress is affected by strain-rate [29]. No suitable correction has been formulated for round specimens under these conditions let alone for flat specimens where the stress field is more complex. The triaxial stress state as well as strain-induced hardening could cause erroneous values of m to be obtained in change-rate tests. However, results related to the anisotropy of superplastic flow [4, 5] indicate that the change rate method may still be very sensitive to the effect of small changes in metallurgical variables on peak values of m provided that rate changes are performed in the same sequence and at equivalent strains in each testing sequence. It is also evident that in most discussions of m a

TABLE III Effect of strain-rate and elongation on internal and applied stresses.

Strain rate	Elongation, %	σ_{app}(MN/m^2)	σ_I(MN/m^2)	α_I/σ_{app}
4.2×10^{-1} min.$^{-1}$	100	6.48	0.42	0.065
	200	6.0	0.58	0.097
4.2 min.$^{-1}$	100	15.3	0.73	0.048
	200	15.8	0.70	0.044

comparative rather than absolute value is required so that these problems are largely eliminated. A more satisfactory method for determining m, over a range of strain-rates on only one specimen, may be the stress relaxation test [30] where the total strain need only be of the order of 1 to 2% thus substantially reducing the effects of strain-hardening and necking. This method would, however, usually require special instrumentation for high speed load measurement.

The magnitudes of internal stresses were determined by the stress relaxation technique [21] at 100 and 200% elongation for initial strain-rates of 4.2×10^{-1} min.$^{-1}$ and 4.2 min.$^{-1}$. Results presented in table III indicate that at both strain-rates the internal stress, σ_I, is only a small proportion of the applied stress so that the effective stress is the major component of the flow stress. The internal stress is smaller at the lower strain-rate than at the faster strain-rate but is a greater proportion of the applied stress, σ_{app}, at the lower rate. Increase of σ_I with elongation at the lower strain-rate may indicate that strain hardening is not balanced by recovery effects at strain-rates close to where m (as indicated by the $\log\sigma - \log\epsilon$ slope) is a maximum. The constancy of the internal stress at the faster strain-rate of 4.2 min.$^{-1}$ indicates that a steady state situation of strain-hardening balanced by recovery, is reached prior to 100% elongation at this strain-rate. These results are compatible with observations of a stacking fault substance in the α phase after deformation at strain-rates of about 10^{-1} min^{-1} and also the formation of dislocation tangles and cells at the fast rate [5].

Elongation at fracture for a number of initial strain-rates is shown in fig. 7. Included in this plot are two points resulting from tests not taken to fracture. Maximum elongation occurs at an intermediate strain-rate range which is somewhat lower than the strain-rate at which $m(\log\sigma - \log\dot{\epsilon}$ slope, fig. 4) is a maximum. This is more clearly shown in fig. 8 where elongation is

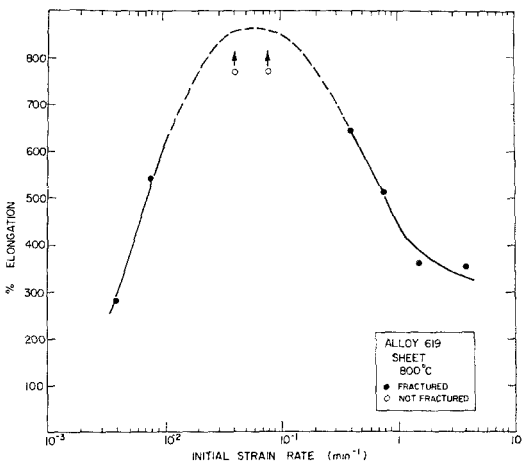

Figure 7 Elongation at fracture for a number of initial strain-rates.

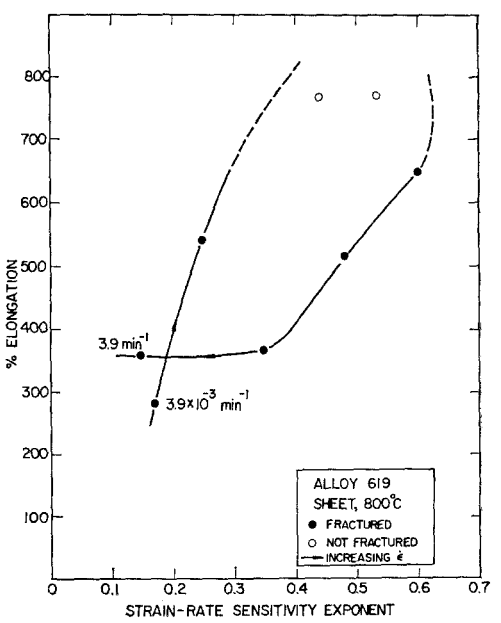

Figure 8 The same data as fig. 7 replotted as a function of m.

replotted as a function of m. Three reasons may be advanced to explain this behaviour:

(i) The strain-rate along the gauge length of the necked specimen varies with both distance from the root of the neck and elongation so that the shape of the neck and subsequent elongation at fracture does not depend simply on a particular value of m associated with the initial strain-rate.

(ii) The onset of the second stage of necking, which Wray [14] found to lead to intrinsic plastic failure, may not be solely dependent on m but is likely to depend significantly on other variables such as strain-rate, strain hardening and the amount of cavitation taking place.

(iii) Cavitation occurs at interfaces between phases in Alloy 619 at strain-rates greater than 7.9×10^{-2} min^{-1} and the amount of cavitation increases with increasing strain and strain-rate [5]. Ductility is limited by the growth and interlinkage of cavities to give premature failure at strain-rates greater than 10^{-1} min.$^{-1}$ while at lower strain-rates, where cavitation does not occur, final fracture is by intrinsic plastic failure.

Of interest is the observation, recorded in fig. 8, of an elongation at fracture for an initial strain-rate of 3.9 min^{-1} which is greater than for the very much lower initial strain-rate of 3.9×10^{-3} min^{-1}, although similar values of m hold for both strain-rates and although a large amount of cavitation occurs at the fast rate. Of importance here may be an increased rate of strain-hardening which must offset the effect of cavitation, reduce the rate of necking and delay fracture.

3.2 Plate Material

Comparison of figs. 9 and 7 shows that maximum ductility for the plate material occurred in the same strain-rate range as for sheet Alloy 619, and similar values of fracture elongation are obtained. This suggests that the overestimate of elongation in the flat specimens (see experimental section) is within tolerable limits although round specimens would normally be expected to yield highest elongations.

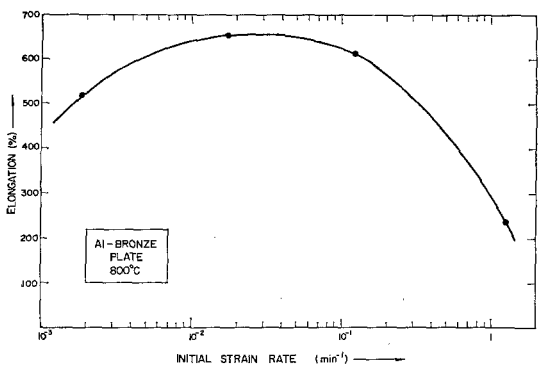

Figure 9 The effect of initial strain-rate on the elongation of plate material.

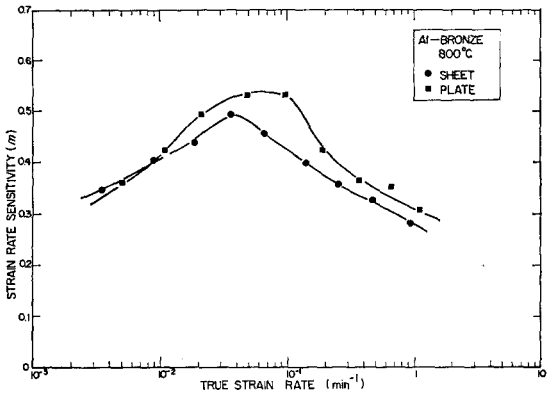

Figure 10 The variation of m with strain-rate as determined by change-rate tests on both sheet and plate material.

Values of m for both plate material and sheet material obtained by change-rate tests are compared in fig. 10. The small differences in these curves probably arise from differences in specimen geometry and stress state during necking. Initial flow stresses for plate material were similar to those for sheet material as may be seen by comparison of the results recorded in table IV with fig. 3.

TABLE IV Variation of maximum engineering stress with strain-rate for plate Alloy 619

Initial strain-rate min.$^{-1}$	Maximum engineering stress MN/m^2
1.8×10^{-3}	0.6
1.8×10^{-2}	2.0
1.8×10^{-1}	5.2
1.8	14.5

These similarities in mechanical behaviour between sheet and round specimens suggests that there is little difference in the nature of superplastic flow of the two forms of Alloy 619. This is expected since both forms have a similar microstructure at 800°C [5]; the point is made because it may be of practical relevance.

One important point in considering the

phenomenological explanation of superplasticity in terms of the strain-rate sensitivity exponent is the position of the strain-rate at the onset of necking upon the $m - \dot{\epsilon}$ curve (e.g. fig. 10). As shown in fig. 5 the local strain-rate at the point of minimum cross-section increases substantially at the onset of plastic instability. If the initial strain-rate is less than that for maximum m then the strain-rate sensitivity will progressively increase and the rate of neck growth will be substantially diminished as compared to a situation on the opposite side of the maximum. Here, even for an identical strain-rate sensitivity, ductility could be lower due to the progressive decrease in strain-rate sensitivity as instability proceeds.

4. Conclusions

1. Alloy 619 can be rendered superplastic at 800°C. Fracture elongations of greater than 700% may be achieved when the initial applied strain-rate is in the range 3.9×10^{-2} min^{-1} to 7.9×10^{-2} min^{-1}. For initial strain-rates either faster or slower than this range the ductility progressively decreases.
2. The tensile strain at the onset of plastic instability in strain-rate sensitive materials is relatively independent of m and is inversely related to the applied strain-rate.
3. In a constant cross-head speed tensile test, at strain-rates where m is high, the local strain-rate at the point of minimum cross-section may increase by about a factor of two after the onset of plastic instability and then steadily decrease to marginally greater than the initial strain-rate after about 200% elongation.
4. Differences may occur between values of m determined by the change-rate method and values of m determined from the slope of a log stress versus log strain-rate plot. These differences are chiefly due to uncertainties in both true strain-rate and the stress state which arise as a result of plastic instability occurring during change-rate testing.
5. The initial strain-rate for maximum elongation of Alloy 619 is lower than the strain-rate for maximum m determined from the slope of a $\log\sigma - \log\dot{\epsilon}$ plot. This may be because peak elongation is associated with a strain-rate sensitivity exponent corresponding to a strain-rate slightly less than that for maximum m.

Acknowledgements

This work was supported by the Defence Research Board and National Research Council of Canada. Discussions with Mr J. Crane of Olin Corporation, who also supplied the material, Dr G. J. Davies and Mr C. P. Cutler of the University of Cambridge are acknowledged with pleasure.

References

1. R. H. JOHNSON, *Metall. Rev.* **15** (1970) 115.
2. G. J. DAVIES, J. W. EDINGTON, C. P. CUTLER, and K. A. PADMANABHAN, *J. Mater. Sci.* **5** (1970) 1091.
3. J. CRANE, Olin Corporation, New Haven, Connecticut, ASM Conference Philadelphia (1969).
4. G. L. DUNLOP and D. M. R. TAPLIN, *Met. Trans.* (1971) (in press).
5. *Idem*, to be published.
6. P. A. BLENKINSOP and J. A. F. GIDLEY, Imperial Metal Industries, Birmingham, Sheet Metal Conference, University of Aston (1969).
7. D. M. R. TAPLIN, G. L. DUNLOP, S. SAGAT, and R. H. JOHNSON, *Proc. II Inter-American Conference on Materials Technology* Mexico City (1970). (ASME, New York), **1** 253.
8. W. A. BACKOFEN, E. R. TURNER, and D. H. AVERY, *Trans. Amer. Soc. Metals* **57** (1994) 980.
9. G. B. GIBBS, *Mater. Sci. Eng.* **2** (1967) 269.
10. A. CONSIDÈRE, "*Ann Ponts et Chaussées*" **9** (1885) Ser. 6, 574.
11. A. NADAI and M. J. MANJOINE, *Trans. ASME* **63** (1941) A77.
12. E. OROWAN, *Reports Progr. Phys.* **12** (1949) 185.
13. J. D. CAMPBELL, *J. Mech. Phys. Solids* **15** (1967) 359.
14. P. J. WRAY, *J. Appl. Phys.* **41** (1970) 3347.
15. T. H. ALDEN, *Trans. Amer. Soc. Metals.* **61** (1968) 559.
16. R. B. NICHOLSON, "Plasticity and Superplasticity", Inst. of Metallurgists, **19** (1970).
17. D. A. WOODFORD, *Trans. Amer. Soc. Metals* **62** (1969) 291.
18. D. H. AVERY and J. M. STUART, Sagamore Army Materials Research Conference. 1967, "Surfaces and Interfaces II" ed. Burke, Reed, and Weiss (Syracuse Univ. Press, New York, 1968) 371.
19. T. Y. M. AL-NAIB and J. L. DUNCAN, *Int. J. Mech. Sci.* **12** (1970) 463
20. W. B. MORRISON, *TMS, AIME* **242** (1968) 2227.
21. D. J. LLOYD and J. D. EMBURY, *Met. Sci. J.* **4** (1970) 6.
22. P. J. MACKEN and A. A. SMITH, "The Aluminium Bronzes" (Copper Development Association, London 1957) 201.
23. J. H. KEELER, *Trans. Amer. Soc. Metals* **47** (1955) 157.
24. D. E. TYLER and R. J. GOODWIN, *J. Inst. Metals* **96** (1968) 314.
25. B. M. WATTS and M. J. STOWELL, *J. Mater. Sci.* **6** (1971) 228.
26. D. E. NEWBURY and D. C. JOY, *Scripta Metallurgica* **4** (1970) 825.
27. T. H. ALDEN, *Acta Metallurgica* **17** (1969) 1435.

28. P. W. BRIDGEMAN, *Trans. Amer. Soc. Metals* **32** (1944) 353.
29. P. J. WRAY and O. RICHMOND, *J. Appl. Phys.* **39** (1968) 5754.
30. D. LEE and E. W. HART, *Met. Trans.* **2** (1971) 1245.

Received 2 August and accepted 13 August 1971.